Laboratory study of the Biermann battery magnetic field compression in laser-produced plasma

Contact: julien.fuchs@polytechnique.edu

W. Yao
LULI - CNRS; École Polytechnique, CEA; Université Paris-Saclay; UPMC Université Paris 06; Sorbonne Université, F-91128, Palaiseau Cedex, France

H. Ahmed
Central Laser Facility, STFC Rutherford Appleton Laboratory, Didcot, UK

P. Antici
INRS-EMT, 1650 boul, Lionel-Boulet, Varennes, QC, J3X 1S2, Canada

J. Béard
LNCMI-T, CNRS, Toulouse, France

M. Borghesi
Center for Plasma Physics, School of Mathematics and Physics, Queen's University Belfast, Belfast BT7 1NN, United Kingdom

A. F. A. Bott
Department of Physics, University of Oxford, Parks Road, Oxford OX1 3PU, UK.

D. C. Carroll
Central Laser Facility, STFC Rutherford Appleton Laboratory, Didcot, UK

S. N. Chen
"Horia Hulubei" National Institute for Physics and Nuclear Engineering, 30 Reactorului Street, RO-077125, Bucharest-Magurele, Romania

A. Ciardi
Sorbonne Université, Observatoire de Paris, Université PSL, CNRS, LERMA, F-75005, Paris, France

C. Fegan
Center for Plasma Physics, School of Mathematics and Physics, Queen's University Belfast, Belfast BT7 1NN, United Kingdom

E. D. Filippov
CLPU, 37185 Villamayor, Spain

E. d'Humières
University of Bordeaux, Centre Lasers Intenses et Applications, CNRS, CEA, UMR 5107, F-33405 Talence, France

R. Lelièvre
LULI - CNRS; École Polytechnique, CEA; Université Paris-Saclay; UPMC Université Paris 06; Sorbonne Université, F-91128, Palaiseau Cedex, France

P. Martin
Center for Plasma Physics, School of Mathematics and Physics, Queen's University Belfast, Belfast BT7 1NN, United Kingdom

A. Sladkov
Light Stream Labs LLC, USA, Palo Alto, CA 94306

S. Pikuz
HB11 Energy Holdings, Freshwater, NSW 2096, Australia

J. Fuchs
LULI - CNRS; École Polytechnique, CEA; Université Paris-Saclay; UPMC Université Paris 06; Sorbonne Université, F-91128, Palaiseau Cedex, France

Abstract

In this work we present experimental results related to the collision of parallel magnetic fields and study the compression that ensues between them. For this, we use two dense, spatially separated, targets that are both irradiated by nanosecond laser beams. The generated magnetic fields due to the Biermann battery effect close to the target surfaces are clockwise with respect to the plasma expansion axis. The ablating plasmas radially expand and advect the aligned parallel magnetic fields to the interaction region between the targets. By shifting the targets along their normal, we enable these laterally expanding Biermann fields to collide, leading to magnetic field compression and accumulation in the gap between the targets. To resolve in time the topology of the compressed magnetic field we employ the proton deflectometry technique to diagnose each magnetic field and the magnetic field pile-up between the targets.

1 Introduction

Magnetic energy is an universal source of energy in the cosmos and plays a crucial role in astrophysical processes such as jet formations [1], gamma-ray bursts [2], magnetic reconnection [3] and so on, as well as in laboratory plasma experiments on Inertial Confinement Fusion (ICF). Generation and compression of strong magnetic fields is a rapidly developing area of High-Energy-Density-Physics (HEDP), with a significant interest be-

ing associated with the magneto-inertial approach used by the fusion community [4]. The implementation of the regime of magnetized fusion requires using extremely strong magnetic fields, exceeding 1000 T. Obtaining such strenghts of magnetic fields in the laboratory is possible by compressing them from the seed field which can be induced by an external generator [5], [6] or from self-generated in laser produced plasmas [7], [8]. Self-generation can arise from one of the recognized mechanisms such as Biermann battery [9] due to noncollinear temperature and density gradients or kinetic Weibel instability [10] arising from anisotropic distribution functions [11]–[13] or beamlike distributions [14], [15].

In this work, we present the results of an experiment conducted with colliding parallel magnetic fields. In such a configuration, the reconnection is canceled out and we can follow the compression of the self-generated magnetic fields. The experiment uses two thin copper targets displaced along the normal to the target surface direction. Both are irradiated by high power laser beams of ns-scale duration (Fig. 1). As the plasmas radially expand from the laser spots, they drive aligned magnetic fields between the targets. Such configuration has already been tested [16], the proton radiography showed the "overlapping" of two magnetic structures, and low-level enhancement of the magnetic flux due to the collision. In order to observe noticeable increase of the magnetic field we followed latter times (> 2 ns) and reduced the distance between the targets (< 0.5 mm), as we expect that the maximal strength of magnetic field is compressed against the dense target due to the Nernst effect [17], [18]. The experiment allows us, by varying the gap between the target surfaces, to measure the optimal distance for the effective compression. In the work, for convenience, we denote the distance between the target surfaces as the α parameter.

2 Experiments

2.1 Setup

This experiment was carried out at the Vulcan Target Area West (TAW) laser facility at the Rutherford Appleton Laboratory (RAL). The top view of the experimental setup is shown in Fig. 1. Two 5 μm thick copper targets (T1 and T2) were irradiated by two laser beams (L1 and L2, having ~ 35 GW power over a duration of 1.4 ns (Gaussian FWHM), and focused over an averaged radii of ~ 25 μm circular focal spots, yielding on-target intensity of $\sim 10^{15}$ W/cm^2). The laser irradiation on the two targets generated two hot, dense plasmas that expand radially toward each other. Regarding the separation between the two targets, we note that, as previously recorded [17] using similar laser conditions, the radial magnetic field expansion is ~ 300 μm/ns. Therefore, we chose the separation between the two laser impacts to be, along the x-axis, $\delta = 500$ μm (see Fig. 1),

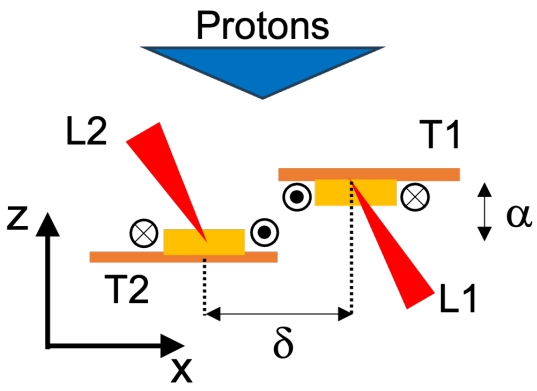

Figure 1: **Scheme of the experimental setup performed at the TWA area of Vulcan.** α is the distance (along the proton beam axis) between the two targets. Schematic diagram of the experiment in the xz-plane, using two lasers (L1 and L2, separated along the x-axis by $\delta = 500$ μm) and two targets (T1 and T2, separated along the x-axis by a variable distance α). Also shown are the protons (in light blue, sent along the z-axis) used for the radiography diagnostic and the plasma plume with frozen-in magnetic flux tube generated by each laser ablation at the target front (in yellow).

such that there is some overlap between the two magnetic flux tubes within the first ns of the magnetic field generation.

We will now focus on the characterization of the individual magnetic field structures produced by each plasma.

2.2 Proton radiography results

The primary diagnostic used to characterize each magnetic field in strength and spatial distribution in the xy-plane, as well as the encounter of the two magnetic fields, is proton radiography [19]. This diagnostic uses fast, laminar protons, induced by the auxiliary high-intensity laser beam B8 [20]. A short pulse laser capable of delivering ~ 150J, $\sim 10^{19}$ W/cm^2 was incident on 25 μm gold targets to create a broadband, divergent proton beam through the TNSA mechanism. A radiochromic film (RCF) stack consisting of layers of Gafchromic HDV2 and EBT3 was used as the radiography detector. The distance between the proton source and the midpoint between the T1 and T2 targets was 9.66 mm. Additionally, the distance between the copper targets and the RCF stack was 90 mm giving a geometric magnification of ~ 10.3. Separate RCFs of the same type were calibrated by physicists of the CLF, using the University of Birmingham cyclotron. Through scanning the calibrated and experimental RCFs on the same scanner (EPSON Precision 2450), a model relating the optical density and dose was determined allowing all experimental RCFs to

be converted into proton-deposited dose.

Here, the protons are sent along the z-axis, as illustrated in Fig. 1. As they propagate through the target assembly and the magnetic fields, the protons are deflected, following which they are collected on films (RCF) that record the path-integrated (along the z-axis) deflections. The principle of the diagnostic is that analyzing the deflectometry patterns yields information on the fields encountered along their way by the probing protons.

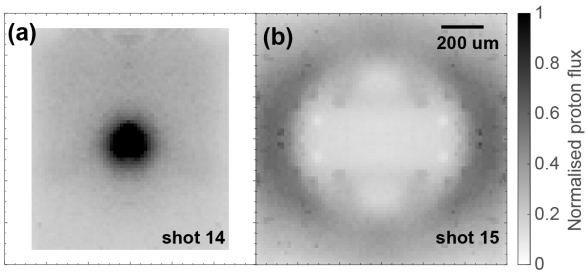

Figure 2: **Proton radiography results** Experimental RCF measurements probing the single magnetic flux tubes produced on (a) target T2 or (b) target T1. Both images are snapshots taken at at 1 ns.

The experimental films shown in Fig. 2 display the dose modulations recorded by 6.6 MeV protons of the magnetic fields on a single T2 target (a) and on a single T1 target (b). As the direction of the magnetic fields from the two targets relative to the probing proton beam are opposite (see Fig. 1), therefore these magnetic fields affect the probing proton beam in opposite ways. When there is only a plasma expanding from the T2 target, the magnetic field structure focuses the proton beam, leading to a concentrated proton dose (see Fig. 2 (a)), as expected [21], [22]. Conversely, and also as expected [21], [22], the proton deflection pattern is reversed when there is only a plasma expanding from the T1 target, i.e. the magnetic field structure now defocuses the proton beam, yielding a radiograph characterized by a large white ring structure surrounded by a dark ring, the probing protons having been expelled from within, and to be accumulated at the edge (see Fig. 2 (b)).

We will further quantify the above analyse of the proton radiography results with the code PROBLEM [23].

3 Analysis

Figure 3 displays the path-integrated magnetic field map, reconstructed from the proton deflectometry map shown in Fig. 2, using the PROBLEM algorithm [24]. From Fig. 3 (a) and (b), we can see that the magnetic fields generated from the two single shots are similar to each other, which serves as a benchmark of our methodology.

With the above mentioned analysis tool benchmarked,

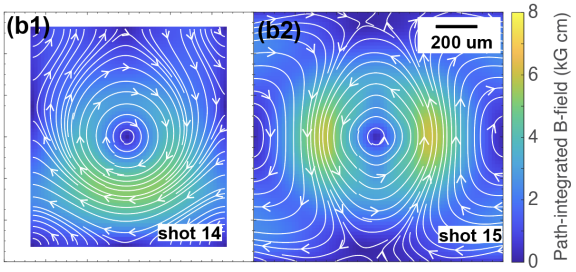

Figure 3: **Analysis of the RCF results.** Path-integrated magnetic field strength analyzed via the code PROBLEM [24]. The white-arrow streamlines represent the in-plane magnetic field lines (B_x and B_y), and the colormap shows the path-integrated (along the z-axis) strength of the xy-plane magnetic field.

we will start to analyse the shots taken when we have used both laser beams and check the magnetic field compression between them in a quantitative manner.

4 Conclusion

In summary, we have set a platform to systematically investigate the magnetic field compression that can take place when two independent magnetic flux tubes are encountering. Our proton radiography diagnostics can clearly quantify the magnetic field maps in the interaction region. By using the PROBLEM code, we will be able to quantify this compression with our data as a function of time and separation distance (i.e., α). More detailed characterization of the local plasma conditions are also underway (with additional diagnostics like optical interferometry and Thomson scattering), together with three-dimensional numerical simulations to reveal the underlying physics.

References

[1] B. Albertazzi, A. Ciardi, M. Nakatsutsumi, *et al.*, "Laboratory formation of a scaled protostellar jet by coaligned poloidal magnetic field," *Science*, vol. 346, no. 6207, pp. 325–328, 2014.

[2] R. W. Klebesadel, I. B. Strong, and R. A. Olson, "Observations of gamma-ray bursts of cosmic origin," *Astrophysical Journal, vol. 182, p. L85*, vol. 182, p. L85, 1973.

[3] M. Hesse and P. Cassak, "Magnetic reconnection in the space sciences: Past, present, and future," *Journal of Geophysical Research: Space Physics*, vol. 125, no. 2, e2018JA025935, 2020.

[4] M. R. Gomez, S. A. Slutz, A. B. Sefkow, *et al.*, "Experimental demonstration of fusion-relevant conditions in magnetized liner inertial fusion," *Physical review letters*, vol. 113, no. 15, p. 155 003, 2014.

[5] O. Gotchev, P. Chang, J. Knauer, *et al.*, "Laser-driven magnetic-flux compression in high-energy-density plasmas," *Physical review letters*, vol. 103, no. 21, p. 215 004, 2009.

[6] D. Nakamura, A. Ikeda, H. Sawabe, Y. Matsuda, and S. Takeyama, "Record indoor magnetic field of 1200 t generated by electromagnetic flux-compression," *Review of Scientific Instruments*, vol. 89, no. 9, p. 095 106, 2018.

[7] K. M. Schoeffler, N. F. Loureiro, R. Fonseca, and L. Silva, "Magnetic-field generation and amplification in an expanding plasma," *Physical review letters*, vol. 112, no. 17, p. 175 001, 2014.

[8] C. Huntington, F. Fiuza, J. Ross, *et al.*, "Observation of magnetic field generation via the weibel instability in interpenetrating plasma flows," *Nature Physics*, vol. 11, no. 2, pp. 173–176, 2015.

[9] L. Biermann and A. Schlüter, "Cosmic radiation and cosmic magnetic fields. ii. origin of cosmic magnetic fields," *Physical Review*, vol. 82, no. 6, p. 863, 1951.

[10] E. S. Weibel, "Spontaneously growing transverse waves in a plasma due to an anisotropic velocity distribution," *Physical Review Letters*, vol. 2, no. 3, p. 83, 1959.

[11] R. Morse and C. Nielson, "Numerical simulation of the weibel instability in one and two dimensions," *The Physics of Fluids*, vol. 14, no. 4, pp. 830–840, 1971.

[12] D. Romanov, V. Y. Bychenkov, W. Rozmus, C. Capjack, and R. Fedosejevs, "Self-organization of a plasma due to 3d evolution of the weibel instability," *Physical review letters*, vol. 93, no. 21, p. 215 004, 2004.

[13] C. Zhang, Y. Wu, M. Sinclair, *et al.*, "Mapping the self-generated magnetic fields due to thermal weibel instability," *Proceedings of the National Academy of Sciences*, vol. 119, no. 50, e2211713119, 2022.

[14] F. Califano, F. Pegoraro, and S. Bulanov, "Impact of kinetic processes on the macroscopic nonlinear evolution of the electromagnetic-beam-plasma instability," *Physical Review Letters*, vol. 84, no. 16, p. 3602, 2000.

[15] L. O. Silva, R. A. Fonseca, J. W. Tonge, W. B. Mori, and J. M. Dawson, "On the role of the purely transverse weibel instability in fast ignitor scenarios," *Physics of Plasmas*, vol. 9, no. 6, pp. 2458–2461, 2002.

[16] M. Rosenberg, C. Li, W. Fox, *et al.*, "First experiments probing the collision of parallel magnetic fields using laser-produced plasmas," *Physics of Plasmas*, vol. 22, no. 4, p. 042 703, 2015.

[17] L. Lancia, B. Albertazzi, C. Boniface, *et al.*, "Topology of megagauss magnetic fields and of heat-carrying electrons produced in a high-power laser-solid interaction," *Physical review letters*, vol. 113, no. 23, p. 235 001, 2014.

[18] L. Gao, P. Nilson, I. Igumenshchev, *et al.*, "Precision mapping of laser-driven magnetic fields and their evolution in high-energy-density plasmas," *Physical review letters*, vol. 114, no. 21, p. 215 003, 2015.

[19] D. B. Schaeffer, A. F. A. Bott, M. Borghesi, *et al.*, *Proton imaging of high-energy-density laboratory plasmas*, 2022. DOI: 10.48550/ARXIV.2212.08252. [Online]. Available: https://arxiv.org/abs/2212.08252.

[20] R. A. Snavely, M. H. Key, S. P. Hatchett, *et al.*, "Intense high-energy proton beams from petawatt-laser irradiation of solids," *Physical Review Letters*, vol. 85, no. 14, pp. 2945–2948, Oct. 2000. DOI: 10.1103/physrevlett.85.2945. [Online]. Available: https://doi.org/10.1103/physrevlett.85.2945.

[21] C. Cecchetti, M. Borghesi, J. Fuchs, *et al.*, "Magnetic field measurements in laser-produced plasmas via proton deflectometry," *Physics of Plasmas*, vol. 16, no. 4, p. 043 102, 2009.

[22] R. D. Petrasso, C. K. Li, F. H. Seguin, *et al.*, "Lorentz mapping of magnetic fields in hot dense plasmas," *Physical Review Letters*, vol. 103, no. 8, Aug. 2009. DOI: 10.1103/physrevlett.103.085001. [Online]. Available: https://doi.org/10.1103/physrevlett.103.085001.

[23] A. Bott, C. Graziani, P. Tzeferacos, *et al.*, "Proton imaging of stochastic magnetic fields," *Journal of Plasma Physics*, vol. 83, no. 6, p. 905 830 614, 2017.

[24] A. Bott, C. Graziani, P. Tzeferacos, *et al.*, "Proton imaging of stochastic magnetic fields," *Journal of Plasma Physics*, vol. 83, no. 6, p. 905 830 614, 2017.